JOC Article

Probing Electronic Communication in Stable Benzene-Bridged Verdazyl Diradicals

Joe B. Gilroy,[†] Steve D. J. McKinnon,[†] Pierre Kennepohl,[‡] Mark S. Zsombor,[†] Michael J. Ferguson,[§] Laurence K. Thompson,[||] and Robin G. Hicks*,[†]

Department of Chemistry, University of Victoria, P.O. Box 3065, Victoria, BC, Canada V8W 3V6, Department of Chemistry, The University of British Columbia, 2036 Main Mall, Vancouver BC, Canada V6T 1Z1, Crystallography Laboratory, Department of Chemistry, University of Alberta, 11227 Saskatchewan Dr. NW, Edmonton, Alberta, Canada T6G 2G2, and Department of Chemistry, Memorial University, St. John's, Newfoundland, Canada A1B 3X7

rhicks@uvic.ca

Received July 3, 2007

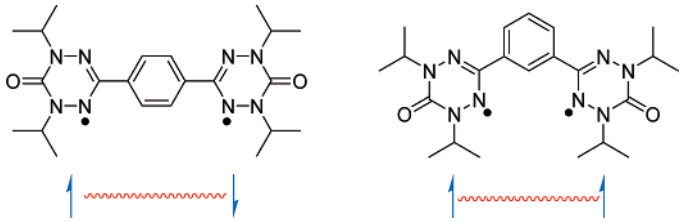

Two benzene-bridged *N*,*N*′-bis(isopropyl)6-oxoverdazyl diradicals **7a** (1,4-benzene-bridged) and **7b** (1,3-benzene-bridged) were prepared and studied by an array of physicochemical techniques aimed at elucidating the intramolecular electronic and magnetic coupling between verdazyl chromophores. The very high stability of these diradicals permits comprehensive investigations of their properties for the first time. The UV−vis spectra suggest negligible direct conjugative overlap involving the radical SOMOs, although significant differences in higher energy absorptions suggest that radical orbitals other than the SOMO are likely communicating via the central *p*-phenylene bridge in **7a**. The electrochemical features of the two diradicals are nearly identical; in each derivative, both radicals are oxidized essentially independently while the reductions occur in a stepwise manner with differences of ∼100mV between the two reductions. EPR and magnetic susceptibility collectively indicate that the para-bridged diradical is weakly antiferromagnetically coupled while the meta analogue is weakly ferromagnetically coupled, in accord with the topology of the substitution pattern on the central benzene ring.

Introduction

Investigations of the electronic properties of π-conjugated organic diradicals have been of long-standing interest.[1,2] Much of the early work focused on reactive diradicals based on, e.g., substituted methyl radicals, carbenes, and nitrenes as the spin carriers,[2,3] but studies on stable[4] (isolable) diradicals have now become quite common; in addition to ongoing fundamental interest, the latter systems offer significant practical advantages as models and building blocks for organic magnetic materials.[5,6]

Among diradicals constructed from stable radical species, those based on nitroxides[7−10] and related radicals have, not surprisingly, dominated—although other paramagnetic centers (semiquinones,[11,12] triarylmethyl[13] radicals) have also received

[†] University of Victoria.
[‡] The University of British Columbia.
[§] University of Alberta.
[||] Memorial University.

(1) Salem, L.; Rowland, C. *Angew. Chem., Int. Ed.* **1972**, *11*, 92.
(2) *Diradicals*; Borden, W. T., Ed; John Wiley & Sons, Inc.: New York, 1982.
(3) (a) Platz, M. S.; McBride, J. M.; Little, R. D.; Harrison, J. J.; Shaw, A.; Potter, S. E.; Berson, J. A. *J. Am. Chem. Soc.* **1976**, *98*, 5725. (b) Seeger, D. E.; Lahti, P. M.; Rossi, A. R.; Berson, J. A. *J. Am. Chem. Soc.* **1986**, *108*, 1251. (c) Berson, J. A. *Acc. Chem. Res.* **1997**, *30*, 238. (d) Nakamura, N.; Inoue, K.; Iwamura, H.; Fujioka, T.; Sawaki, Y. *J. Am. Chem. Soc.* **1992**, *114*, 1484. (e) Matsuda, K.; Nakamura, N.; Takahashi, K.; Inoue, K.; Koga, N.; Iwamura, H. *J. Am. Chem. Soc.* **1995**, *117*, 5550. (f) Dougherty, D. A. *Acc. Chem. Res.* **1991**, *24*, 88. (g) Minato, M.; Lahti, P. M. *J Phys Org. Chem.* **1993**, *6*, 483. (h) Kalgutkar, R. S.; Lahti, P. M. *J. Am. Chem. Soc.* **1997**, *119*, 4771.
(4) Hicks, R. G. *Org. Biomol. Chem.* **2007**, *5*, 1321.
(5) Rajca, A. *Chem. Rev.* **1994**, *94*, 871.
(6) *Magnetic Properties of Organic Materials*; Lahti, P. M., Ed.; Marcel Dekker, Inc.: New York, 1999.

10.1021/jo7014449 CCC: $37.00
Published on Web 09/21/2007

attention. A good qualitative and, in some cases, quantitative picture of the relationships has been developed between the nature of the π-conjugated "spacer" which links the two radicals and the nature and magnitude of the interactions between spins.[5] By far the best studied spacers are *m*- and *p*-phenylene; meta-substituted diradicals possess high spin ($S = 1$) ground states while para diradicals are generally low spin ($S = 0$). However, the general guidelines are by no means universal as exceptions have been reported.[12,14]

Verdazyl radicals (**1**; X = H_2, O, S) are another established family of stable radicals. Several verdazyl-based diradicals have been reported, though in many cases the results are incomplete or incorrect. A variety of studies on the *p*- and *m*-phenylene-bridged *N*,*N*-diphenylverdazyls **(2a** and **2b**, respectively) provide only a qualitative assessment of weakly interacting spins,[15] while the only attempt to quantify the magnetic interactions between verdazyls in these derivatives[16] incorrectly[17] concluded that both were strongly ferromagnetically coupled diradicals. More recently, Fox et al. prepared a series of *N*,*N*-dimethyl-6-oxoverdazyls **3**, but investigations of the electronic properties of these diradicals were severely compromised by their relatively poor stability.[18] Stability problems were also barriers to the full characterization of directly fused verdazyls **4a**[19] and **4c**.[18] The "oxoverdazyl" analogue **4b** was sufficently stable to be characterized magnetically;[20] this species is a ground-state singlet, with an exchange interaction parameter (determined from variable temperature EPR data) $J = -760$ cm^{-1}. Computational studies on **4b** and **4c** are in good qualitative agreement with the experimentally determined spin-state energetics.[21]

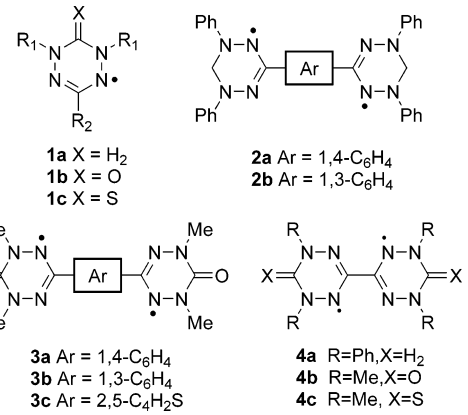

Recent synthetic advances have led to the incorporation of isopropyl groups on the two nitrogen substituents of oxoverdazyls **1b**.[22] These derivatives are much more stable than the corresponding *N*,*N*′-dimethyl derivatives, thus opening up the possibility of making more stable analogues of some of the unstable verdazyl diradicals described above. Thus far, the only such example is methylene-bridged diradical **5** which has a nonconjugated spacer (but nonetheless possesses a strong singlet−triplet gap of −150 cm^{-1}).[23] Herein, we describe the synthesis and comprehensive characterization of 1,4- and 1,3-benzene-bridged *N*,*N*′-diisopropyl-6-oxoverdazyls.

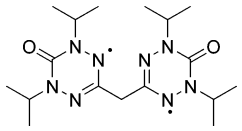

5

Results

Synthesis. The *p*- and *m*-phenylene-bridged verdazyl diradicals (**7a** and **7b**, respectively) were prepared by adaptation of established procedures for the synthesis of *N*,*N*′-diisopropyl-6-oxoverdazyls (Scheme 1).[22] Reaction of 2 equiv of carbonic acid bis(1-isopropyl hydrazide) with the appropriate benzenebis-(carboxaldehyde) in refluxing methanol afforded the bis-tetrazanes **6a** and **6b**. The tetrazanes were then oxidized with 3 equiv of *p*-benzoquinone in refluxing toluene to give verdazyl diradicals **7a** and **7b**. For comparison purposes, a phenyl-substituted verdazyl monoradical **9** was also prepared analogously (Scheme 2). All three verdazyl species are extremely stable, and all were readily established to be analytically pure

(7) (a) Stroh, C.; Turek, P.; Ziessel, R. *Chem. Commun.* **1998**, 2337. (b) Hase, S.; Shiomi, D.; Sato, K.; Takui, T. *J. Mater. Chem.* **2001**, *11*, 756. (c) Schatzschneider, U.; Weyhermuller, T.; Rentschler, E. *Eur. J. Inorg. Chem.* **2001**, 2569. (d) Rajadurai, C.; Ivanova, A.; Enkelmann, V.; Baumgarten, M. *J. Org. Chem.* **2003**, *68*, 9907. (e) Wautelet, P.; Le Moigne, J.; Videva, V.; Turek, P. *J. Org. Chem.* **2003**, *68*, 8025. (f) Hayakawa, K.; Shiomi, D.; Ise, T.; Sato, K.; Takui, T. *Chem. Lett.* **2004**, *33*, 1494. (g) Ziessel, R.; Stroh, C.; Heise, H.; Kohler, F. H.; Turek, P.; Claiser, N.; Souhassou, M.; Lecomte, C. *J. Am. Chem. Soc.* **2004**, *126*, 12604. (h) Zoppellaro, G.; Enkelmann, V.; Geies, A.; Baumgarten, M. *Org. Lett.* **2004**, *6*, 4929. (i) Zoppellaro, G.; Geies, A.; Enkelmann, V.; Baumgarten, M. *Eur. J. Org. Chem.* **2004**, 2367. (j) Stroh, C.; Ziessel, R.; Raudaschl-Sieber, G.; Kohler, F. H.; Turek, P. *J. Mater. Chem.* **2005**, *15*, 850.

(8) Shultz, D. A.; Boal, A. K.; Lee, H.; Farmer, G. T. *J. Org. Chem.* **1999**, *64*, 4386.

(9) Catala, L.; Le Moigne, J.; Kyritsakas, N.; Rey, P.; Novoa, J. J.; Turek, P. *Chem. Eur. J.* **2001**, *7*, 2466.

(10) Hayakawa, K.; Shiomi, D.; Ise, T.; Sato, K.; Takui, T. *J. Mater. Chem.* **2006**, *16*, 4146.

(11) (a) Shultz, D. A.; Boal, A. K.; Farmer, G. T. *J. Org. Chem.* **1998**, *63*, 9462. (b) Shultz, D. A.; Lee, H. Y.; Fico, R. M. *Tetrahedron* **1999**, *55*, 12079. (c) Shultz, D. A.; Bodnar, S. H.; Lee, H.; Kampf, J. W.; Incarvito, C. D.; Rheingold, A. L. *J. Am. Chem. Soc.* **2002**, *124*, 10054. (d) Shultz, D. A.; Fico, R. M.; Bodnar, S. H.; Kumar, R. K.; Vostrikova, K. E.; Kampf, J. W.; Boyle, P. D. *J. Am. Chem. Soc.* **2003**, *125*, 11761.

(12) Shultz, D. A.; Fico, R. M.; Lee, H.; Kampf, J. W.; Kirschbaum, K.; Pinkerton, A. A.; Boyle, P. D. *J. Am. Chem. Soc.* **2003**, *125*, 15426.

(13) (a) Rajca, A.; Utamapanya, S.; Xu, J. T. *J. Am. Chem. Soc.* **1991**, *113*, 9235. (b) Rajca, A.; Rajca, S.; Desai, S. R. *J. Chem. Soc., Chem. Commun.* **1995**, 1957. (c) Rajca, A.; Rajca, S. *J. Am. Chem. Soc.* **1996**, *118*, 8121. (d) Rajca, A.; Rajca, S. *J. Chem. Soc., Perkin Trans. 2* **1998**, 1077. (e) Rajca, A.; Shiraishi, K.; Vale, M.; Han, H. X.; Rajca, S. *J. Am. Chem. Soc.* **2005**, *127*, 9014.

(14) (a) Borden, W. T.; Iwamura, H.; Berson, J. A. *Acc. Chem. Res.* **1994**, *27*, 109. (b) Fang, S.; Lee, M. S.; Hrovat, D. A.; Borden, W. T. *J. Am. Chem. Soc.* **1995**, *117*, 6727. (c) Okada, K.; Imakura, T.; Oda, M.; Murai, H.; Baumgarten, M. *J. Am. Chem. Soc.* **1996**, *118*, 3047. (d) Okada, K.; Imakura, T.; Oda, M.; Kajiwara, A.; Kamachi, M.; Yamaguchi, M. *J. Am. Chem. Soc.* **1997**, *119*, 5740. (e) Zhang, G. B.; Li, S. H.; Jiang, Y. S. *J. Phys. Chem. A* **2003**, *107*, 5573. (f) Dei, A.; Gatteschi, D.; Sangregorio, C.; Sorace, L.; Vaz, M. G. F. *J. Magn. Magn. Mater.* **2004**, *272*−*76*, 1083.

(15) (a) Kuhn, R.; Neugebauer, F. A.; Trischmann, H. *Mon. Chem.* **1966**, *97*, 525. (b) Mukai, K.; Azuma, N.; Shikata, H.; Ishizu, K. *Bull. Chem. Soc. Jpn.* **1970**, *43*, 3958. (c) Kopf, P.; Morokuma, K.; Kreilick, R. *J. Chem. Phys.* **1971**, *54*, 105.

(16) Azuma, N.; Ishizu, K.; Mukai, K. *J. Chem. Phys.* **1974**, *61*, 2294.

(17) Koivisto, B. D.; Hicks, R. G. *Coord. Chem. Rev.* **2005**, *249*, 2612.

(18) Fico, R. M.; Hay, M. F.; Reese, S.; Hammond, S.; Lambert, E.; Fox, M. A. *J. Org. Chem.* **1999**, *64*, 9386.

(19) Neugebauer, F. A.; Fischer, H.; Meier, P. *Chem. Ber.-Recl.* **1980**, *113*, 2049.

(20) Brook, D. J. R.; Fox, H. H.; Lynch, V.; Fox, M. A. *J. Phys. Chem.* **1996**, *100*, 2066.

(21) (a)Nagaoka, S.; Mukai, K.; Nagashima, U. *THEOCHEM* **1998**, *455*, 199. (b) Barone, V.; Bencini, A.; Ciofini, I.; Daul, C. *J. Phys. Chem. A* **1999**, *103*, 4275. (c) Green, M. T.; McCormick, T. A. *Inorg. Chem.* **1999**, *38*, 3061. (d) Chung, G.; Lee, D. *Chem. Phys. Lett.* **2001**, *350*, 339. (e) de Graaf, C.; Sousa, C.; Moreira, I. D.; Illas, F. *J. Phys. Chem. A* **2001**, *105*, 11371.

(22) Pare, E. C.; Brook, D. J. R.; Brieger, A.; Badik, M.; Schinke, M., *Org. Biomol. Chem.* **2005**, *3*, 4258.

(23) Brook, D. J. R.; Yee, G. T., *J. Org. Chem.* **2006**, *71*, 4889.

SCHEME 1

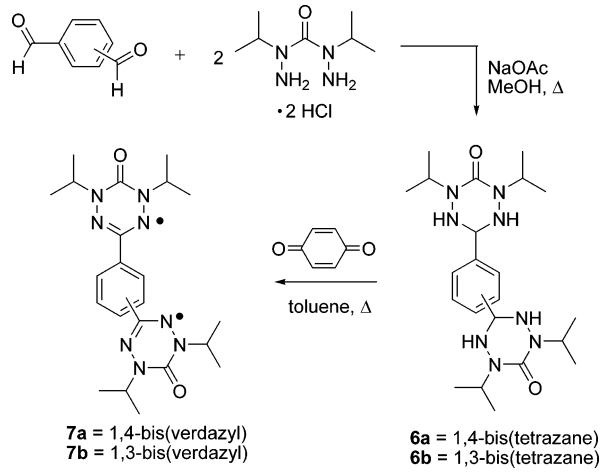

SCHEME 2

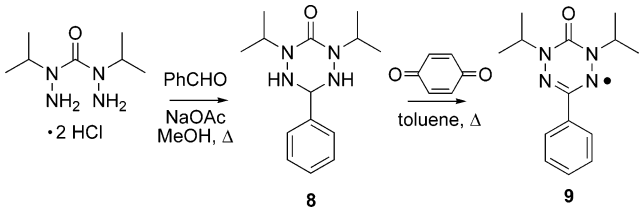

compounds, in contrast to the corresponding *N*,*N*-dimethyl-6-oxoverdazyls (**1b**; R_1 = Me), which can be very long-lived but often decompose too quickly to permit their proper characterization.[18]

Electronic Spectra. The electronic spectra of diradicals **7a**,**b** and monoradical **9** are shown in Figure 1. All three compounds have principal maxima at 417 nm as well as broader, weaker absorptions at 450-470 nm, typical of 3-aryl-6-oxoverdazyl radicals.[24,25] The minor differences between the monoradical and the two diradicals suggest there is limited conjugation between the two verdazyls in **7a** and **7b**. This is not an unexpected finding because the symmetry properties of the verdazyl SOMO (see later) do not permit spin delocalization—and, hence, conjugative overlap—with the phenyl group/spacer in verdazyl mono/diradicals. However, other orbitals (NHOMO, LUMO, etc.) associated with the verdazyl chromophore are likely to be directly conjugated with the phenyl group and have implications for the absorption maxima. This is borne out upon closer inspection of the absorption spectra; the low energy maxima of the 1,4-phenylene diradical **7a** are slightly red-shifted compared to those associated with the 1,3-derivative **7b**, which is consistent with the cross-conjugated relationship between verdazyl centers in the latter. This effect is more pronounced upon examination of the ultraviolet absorptions: monoradical **9** has a UV absorption maximum at 250 nm and the (cross-conjugated) 1,3-diradical **7b** has an absorption at the same wavelength. The corresponding absorption for the 1,4-diradical **7a** is red-shifted to 280 nm.

Electrochemistry. The few existing electrochemical studies of verdazyl radicals[25,26] suggest that these radicals can be reversibly oxidized to cations and irreversibly reduced to anions. Cyclic voltammograms (CVs) of the aromatic-bridged verdazyl diradicals **4a**−**c** possess quasireversible oxidations and reductions which were described as "two-electron" redox processes,[18] though it was not clear how these authors distinguished between a single two-electron process and two simultaneous one-electron transfers. We have carried out electrochemical studies on the three verdazyl species (CV on **7a**, **7b**, and **9**; Osteryoung square wave voltammetry (OSWV) on **7a** and **7b**), and the results are summarized in Table 1. Monoradical **9** possesses quasireversible one-electron oxidation ($E_{1/2}$ = +180 mV vs Fc/Fc^+) and reduction ($E_{1/2}$ = −1380 mV) processes (see the Supporting Information). The ratio of peak intensities is near one for both redox processes, but the differences in peak potentials (ΔE_p) are substantially higher (115 mV for oxidation, 95 mV for reduction) than the ideal expected value of 60 mV.

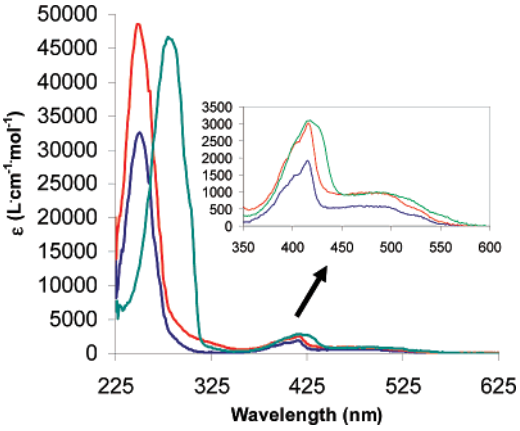

FIGURE 1. Electronic spectra of **7a** (green line), **7b** (red line), and **9** (blue line) in CH_2Cl_2.

TABLE 1. Electrochemical Data for 7a, 7b, and 9 Reported in mV versus Fc/Fc^+

compd	$E_{1/2}^{ox}$ (ΔE_p^{ox})	$E_{1/2}^{red1}$ (ΔE_p^{ox})	$E_{1/2}^{red2}$
7a	+217 (167)	−1337 (N.A.)	−1439 (N.A.)
7b	+215 (175)	−1345 (N.A.)	−1452 (N.A.)
9	180 (115)	−1380 (95)	

The cyclic voltammograms of **7a** and **7b** are shown in Figure 2, and the square wave voltammogram of **7a** is presented in Figure 3. The electrochemical features of the two diradicals are nearly identical to one another; both species can be reversibly oxidized to dications and reduced to dianions. The diradicals have higher oxidation and reduction potentials then the model system **9**, indicating that the verdazyl moiety is slightly withdrawing in nature. The fact that the positioning of the verdazyl radicals relative to one another does not affect their electrochemical properties suggests that the substituent effects are inductive in nature. The CV and OSWV traces clearly demonstrate that the reduction of the diradicals occurs in two sequential one-electron processes, with ~100mV separation between first and second reductions in both cases. In contrast, the oxidations of the two verdazyls in the diradicals occur at, or very close to, the same potentials: both CV and OSWV show the oxidation processes as merged. The peak separations (ΔE_p)

(24) (a) Neugebauer, F. A.; Fischer, H.; Siegel, R. *Chem. Ber. Recl.* **1988**, *121*, 815. (b) Brook, D. J. R.; Fornell, S.; Stevens, J. E.; Noll, B.; Koch, T. H.; Eisfeld, W. *Inorg. Chem.* **2000**, *39*, 562.

(25) Barr, C. L.; Chase, P. A.; Hicks, R. G.; Lemaire, M. T.; Stevens, C. L. *J. Org. Chem.* **1999**, *64*, 8893.

(26) (a) Jaworski, J. S. *J. Electroanal. Chem.* **1991**, *300*, 167. (b) Jaworski, J. S.; Krawczyk, I. *Monatsh. Chem.* **1992**, *123*, 43. (c) Keeney, L.; Hynes, M. J. *Dalton Trans.* **2005**, 133. (d) Chahma, M.; Wang, X. S.; van der Est, A.; Pilkington, M. *J. Org. Chem.* **2006**, *71*, 2750.

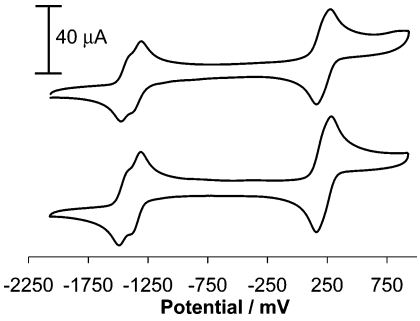

FIGURE 2. Cyclic voltammograms of **7a** (top) and **7b** (bottom) in CH_3CN containing 0.1 M $Bu_4N^+BF_4^-$ (electrolyte). The potential scale is vs the ferrocene/ferrocenium redox couple.

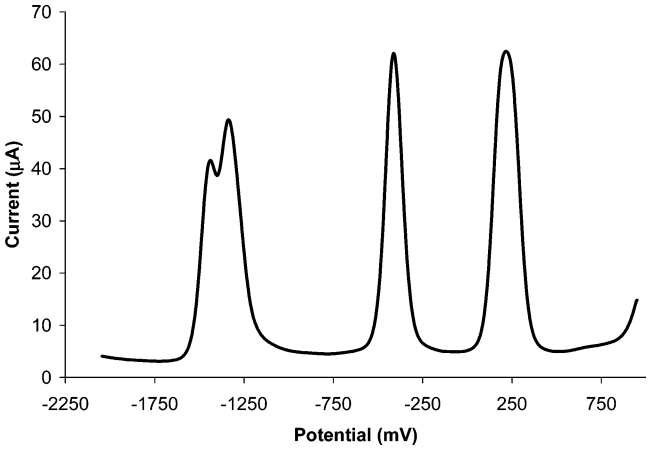

FIGURE 3. OSWV of **7a** in CH_3CN (1 mM) with 0.1 M $Bu_4N^+BF_4^-$ (electrolyte) and 1 mM octamethylferrocene (added as an internal reference: $E_{ox} = -413$ mV vs Fc/Fc^+).

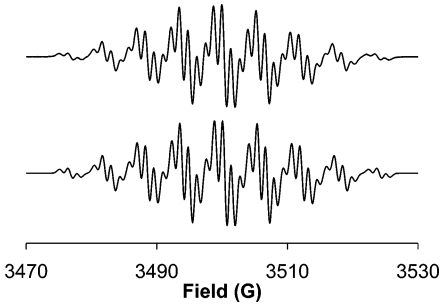

FIGURE 4. X-band EPR spectrum (top) and simulation (bottom) of **9** in CH_2Cl_2.

for the oxidations in the CVs are approximately 170 mV for both diradicals. These values are substantially higher than the ΔE_p value for monoradical **9** and strongly suggests that oxidation of the diradicals occurs as two pseudo-independent one-electron oxidations. A single two-electron oxidation process (as suggested for **4a** and **4b**[18]) is a less likely scenario because the oxidation in the CV in this case would appear as a single wave with a ΔE_p *smaller* than that of a one-electron process (for a reversible Nernstian system, $\Delta E_p = 59/n$ mV at 25 °C where n = number of electrons).

EPR Spectroscopy and Calculations on Monoverdazyl 9. The EPR spectrum of verdazyl **9** (Figure 4) contains a dominant nine-line pattern ($a_{N1,5} = 5.3$ G, $a_{N2,4} = 6.5$G) with additional coupling evident to the methine protons ($a_H = 1.2$ G) of the

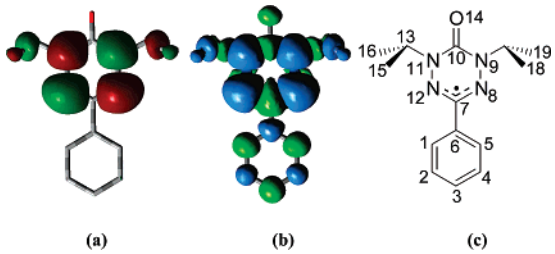

FIGURE 5. (a) Singly occupied molecular orbital, (b) spin density plot, and (c) atom labeling scheme for **9**.

TABLE 2. Atomic Spin Densities for 9

atom	spin density	atom	spin density
C1, C5	−0.029	N9, N11	0.207
C2, C4	0.018	C10	−0.033
C3	−0.027	O14	−0.123
C6	0.032	C13, C17	−0.0123
C7	−0.155	C15, C16, C18, C19	0.0112
N8, N12	0.393		

isopropyl groups. The simulated hyperfine constants agree with those reported in the literature for similar radicals.[22,23]

Computational studies (DFT; B3LYP/6-31G level; see the Supporting Information for details) on **9** were performed to obtain a more complete picture of the spin density distribution in this monoradical, which can be used as a model to understand the spin distributions and the magnetic communication between verdazyls in the diradicals **7a** and **7b.** The verdazyl radical SOMO is well-established[27] as a π^* orbital spanning the four nitrogen atoms (Figure 5a). There are two nodal planes in this orbital, one of which passes through the C7−C8 bond, i.e., the CC bond connecting the verdazyl ring to its C-substituent. As expected, the overall spin densities (Table 2) at the two-coordinate nitrogens (N8, N12; 0.393) and three-coordinate nitrogens (N9, N11; 0.207)—the atoms which constitute the SOMO—are highest. Two other atoms possess significant negative spin density through polarization effects (C7 (−0.155) and O14 (−0.123)). The spin density on C7 in particular is important as it is this position which determines the extent of spin leakage onto the phenyl substituent (which has direct implications for the magnitude of *spin coupling* in the diradicals.[5]) All of the carbon atoms on the phenyl substituent possess spin densities of approximately 0.02−0.03 in magnitude, and the *sign* of the spin density alternates around the ring in the expected way. The *N*-alkyl carbons also possess a small amount (∼0.01) of spin density. Thus, although the dominant spin density sites are those based on the SOMO, spin polarization effects produce non-negligible spin density throughout the radical and, in particular, on the methine carbon of the verdazyl (C7) and the carbonyl oxygen.

EPR of Verdazyl Diradicals. The EPR spectra of diradicals **7a** and **7b** were recorded in toluene glass at 77 K (Figure 6). Both spectra are consistent with randomly oriented triplets.[28] There is very little interference from doublet-based signals (which would be manifested as a single peak in the middle of the spectrum). Analyses of the spectra for **7a** give $g = 2.00488$, $|D/hc| = 0.00210$ cm^{-1}, and $|E/hc| = 0.000047$ cm^{-1}, while

(27) Jornet, J.; Deumal, M.; Ribas-Arino, J.; Bearpark, M. J.; Robb, M. A.; Hicks, R. G.; Novoa, J. J. *Chem. Eur. J.* **2006**, *12*, 3995.

(28) Berson, J. A. In *The Chemistry of Quinonoid Compounds;* Patai, S., Rapoport, Z., Eds.; Wiley: New York, 1988; Vol. II, Chapter 10.

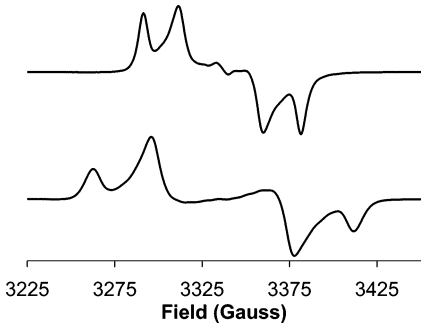

FIGURE 6. X-band EPR spectrum of **7a** (top) and **7b** (bottom) in toluene at 77 K.

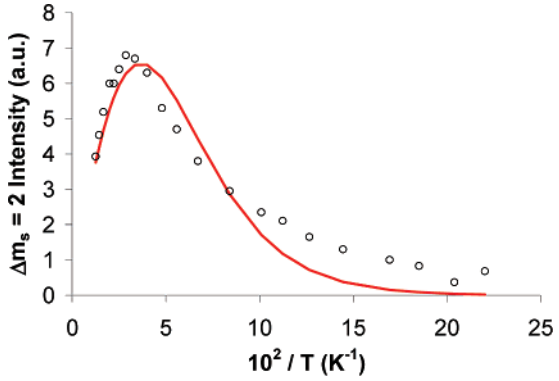

FIGURE 7. Curie plot for **7a** (○) with fit (red line) based on parameters described in text.

7b gives $g = 2.00564$, $|D/hc| = 0.00348$ cm^{-1}, and $|E/hc| = 0.000116$ cm^{-1}. The values of D are inversely proportional to the cube of the interelectronic distance,[28] consistent with the observed values for **7a** and **7b** as the interelectronic distance for the para-substituted diradical should be larger for the meta-substituted diradical.

Variable-temperature EPR data were recorded for **7a** and **7b** in frozen toluene solution by monitoring the triplet half-field signal ($\Delta m_s = 2$) and plotting against inverse temperature (Curie plot). The half-field signal intensity for **7a** showed a nonlinear temperature dependence, which allows for quantitative analysis of the triplet−singlet gap. The Curie plot (Figure 7) was fit using the dimer model (eq 1) based on the spin Hamiltonian ($\mathbf{H} = -J\mathbf{S_1S_2}$)[28,29] (the constant ($C$) is a normalization parameter to account for the arbitrary intensity units). The best fit obtained yields $J = -30.3 \pm 1.4$ cm^{-1}; i.e. **7a** is a ground-state singlet with a relatively weak magnetic interaction. The quality of the fit, though modest at best, is consistent with other examples where the singlet−triplet gap has been evaluated via similar methods.[8]

$$I = \frac{C}{T}\frac{3[\exp(-J/RT)]}{1 + 3[\exp(-J/RT)]} \qquad (1)$$

The analogous variable-temperature EPR analysis for **7b** yielded a linear Curie plot at low temperature (Figure 8). The linearity of this plot is consistent with either a ferromagnetically coupled diradical ($J > 0$) or a degenerate triplet−singlet state ($J = 0$); the EPR data alone do not permit distinction between the two possibilities.[5,28] However, as discussed below, the magnetic susceptibility data are consistent with a triplet ground state for **7b**.

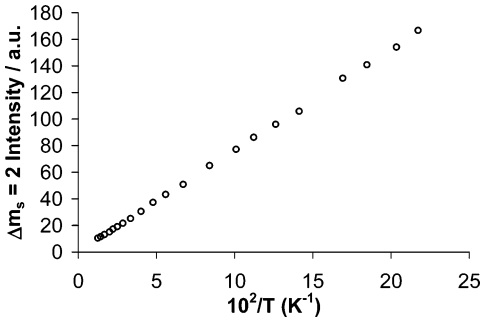

FIGURE 8. Curie plot for **7b**.

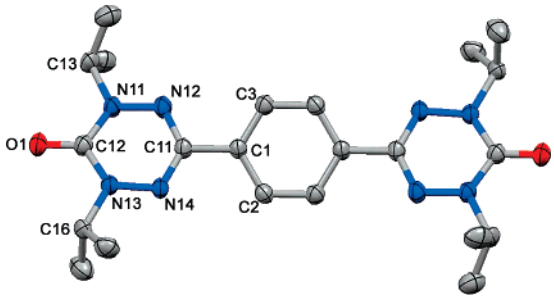

FIGURE 9. Structure of **7a**. Thermal ellipsoids are shown at 50% probability level. Hydrogen atoms removed for clarity. Selected bond lengths (Å): C11−N12 1.329(4), N12−N11 1.368(3), N11−C12 1.371-(4), C12−N13 1.378(4), N13−N14 1.365(3), N14−C11 1.330(4), C12−O1 1.222(3). Selected bond angles (deg): N14−C11−N12 127.0-(2), C11−N12−N11 114.9(2), N12−N11−C12 124.4(2), C12−N13−N14 124.0(2), N13−N14−C11 115.2(2).

Crystal Structures. Diradicals **7a** and **7b** form large crystals upon slow cooling of saturated ethyl acetate solutions. Diradical **7a** crystallizes in the *C*2/*c* space group and has a crystallographic mirror plane passing through the central benzene ring. A thermal ellipsoid plot of **7a** is shown in Figure 9.

The *N*-isopropyl substituents in **7a** are oriented such that the methine protons and the adjacent carbonyl groups are syn with respect to one another. This conformation has been observed in other structurally characterized *N*,*N*′-diisopropyl-6-oxoverdazyls.[30] The two verdazyl rings are twisted by 27.5° relative to the benzene spacer group. The structural metrics of the verdazyl heterocycle are typical for this ring system, and do not support any contribution from quinoidal contributions to electronic structure as is the case for 1,4-diradicals with primary spin density sites directly attached to benzene spacer, e.g., diradical **10**—which is better represented as a closed shell form **10′**.[31]

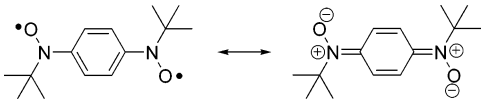

Diradical **7b** crystallizes in the *I*2/*a* space group (Figure 10). All of the *N*-isopropyl groups adopt the same conformation as

(29) Kahn, O. *Molecular Magnetism*; VCH: New York, 1993.

(30) Gilroy, J. B.; Koivisto, B. D.; McDonald, R.; Ferguson, M. J.; Hicks, R. G. *J. Mater. Chem.* **2006**, *16*, 2618.

(31) Nakazono, S.; Karasawa, S.; Koga, N.; Iwamura, H. *Angew. Chem., Int. Ed.* **1998**, *37*, 1550.

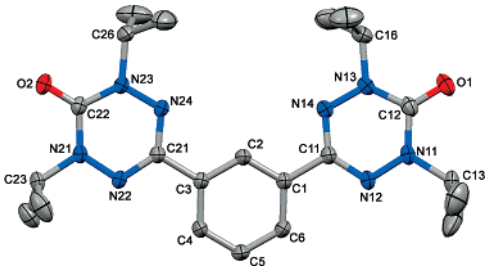

FIGURE 10. Structure of **7b**. Thermal ellipsoids are shown at 50% probability level. Hydrogen atoms removed for clarity. Selected bond lengths (Å): C11−N14 1.3276(14), N14−N13 1.3659(13), N13−C12 1.3770(19), C12−N11 1.376(2), N11−N12 1.3705(16), N12−C11 1.3313(18), C12−O1 1.2229(17), C21−N24 1.3288(18), N24−N23 1.3626(16), N23−C22 1.3777(18), C22−N21 1.3793(18), N21−N22 1.3662(15), N22−C21 1.3276(17), C22−O2 1.2176(16). Selected bond angles (deg): N12−C11−N14 127.06(13), C11−N14−N13 115.05-(12), N14−N13−C12 124.53(12), N13−C12−N11 113.98(12), C12−N11−N12 124.35(12), N11−N12−C11 114.91(12), N22−C21−N24 127.10(12), C21−N24−N23 114.93(11), N24−N23−C22 124.76(12), N23−C22−N21 113.65(11), C22−N21−N22 124.51(11), N21−N22−C21 114.96(11).

was found for **7a**. Both verdazyls are slightly twisted relative to the plane of the central benzene ring: The radical attached at C1 forms a torsion angle of 15.3° with the benzene plane and the radical attached at C3 is twisted by 6.0°. Similarly to the *p*-diradical **7a**, the internal bond lengths and angles of each verdazyl ring are typical. The meta substitution pattern in this diradical precludes the possibility of direct conjugative interactions of the sort described above for **10**.

Magnetic Properties. The magnetic susceptibilities of crystalline samples of **7a** and **7b** were studied between 2 and 300 K. The susceptibility of **7a** (Figure 11) increases as the temperature is lowered and reaches a maximum value at 26 K; upon further cooling the susceptibility drops rapidly before a final, small upturn is observed at cryogenic temperatures. The susceptibility behavior of **7a** was modeled using the Bleaney−Bowers dimer model (eq 2) ($\mathbf{H} = -J\mathbf{S_1S_2}$)[29,32] which was modified with an additional term to account for doublet impurities (eq 2).[29] Fitting the data with a fixed value of $g = 2.00$ yielded $\rho = 0.99$ and $J = -29.73 \pm 0.03$ cm^{-1} (agreement factor $R = 0.0001$; $R = [\Sigma(\chi_{obs} - \chi_{calc})^2/\Sigma\chi_{obs}^2]^{1/2}$); i.e., the two spins in para-substituted diradical **7a** are weakly antiferromagnetically coupled.

$$\chi = \rho\frac{2Ng^2\beta^2}{kT[3 + \exp(-J/kT)]} + (1 - \rho)\frac{Ng^2\beta^2}{3kT}\sum S(S + 1) \quad (2)$$

The magnetic properties of **7b** are shown in Figure 12 in the form of a χT vs T plot. The room-temperature value of 0.832 emu·K/mol is higher than the expected value for noninteracting spins, suggesting the presence of ferromagnetic interactions. As the temperature is lowered, χT increases, reaching a maximum value of 1.44 emu·K/mol at 9 K before decreasing again at lower temperatures. The maximum χT value is significantly greater than the theoretical maximum value of 1.00 emu·K/mol that can be achieved by an $S = 1$ spin system in the absence of other contributions to the susceptibility. This finding implicates ferromagnetic interactions between the verdazyl spins within each diradicals *as well as intermolecular* ferromagnetic interactions contributing to the observed magnetism. However, there

(32) Bleaney, B.; Bowers, K. D. *Proc. R. Soc. London* **1952**, *A214*, 451.

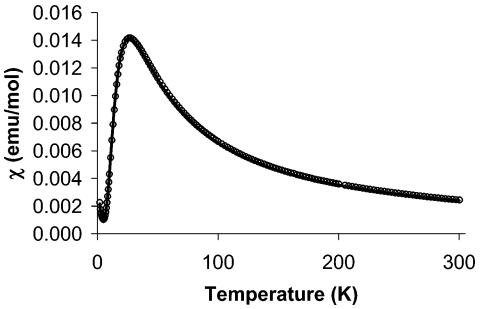

FIGURE 11. Temperature dependence of χ for **7a**. The solid line corresponds to optimal fit using the parameters described in the text.

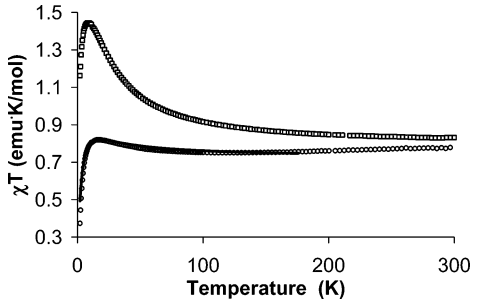

FIGURE 12. Temperature dependence of χT for **7b** (□), diluted in PVC (○), and data fit (line).

must *also* be intermolecular *antiferromagnetic* interactions because χT ultimately decreases at cryogenic temperatures. Modeling such a complex network of magnetic interactions is problematic—even if the "correct" spin model could be constructed and formulated, optimization of this many exchange parameters (at least three) can lead to multiple solutions. Inspection of the solid-state packing of this structure (see the Supporting Information) reveals several intermolecular contacts between heavy atoms in the range of 3.5−3.8 Å, which are beyond standard van der Waals contacts but possibly close enough to lead to non-negligible magnetic interactions. It has been noted that the rationalization of magnetic properties of organic molecular crystals on the basis of specific atom−atom contacts is a tenuous endeavor at best.[33]

In order to attenuate the intermolecular contributions to the magnetism of **7b**, the susceptibility of this compound was also studied as a diluted sample in poly(vinyl chloride) (PVC) film; such studies have been employed in attempts to suppress intermolecular magnetic effects.[10] The dilute sample (∼10 wt % of diradical) was prepared by evaporating a solution of **7b** and PVC in dichloromethane. There, χT product increases upon decreasing temperature, reaching a maximum value of 0.82 emu·K·mol^{-1} at 17 K and then decreasing again below this temperature. The decrease in χT implies aggregation of the diradicals in the PVC medium (i.e., the dilution effect is not ideal). The χT vs T plot for the PVC-diluted sample is also presented in Figure 12. The data below 170 K[34] Were fit according to eq 3, i.e., a Bleaney−Bowers dimer model[29,32] (**H**

(33) Deumal, M.; Cirujeda, J.; Veciana, J.; Novoa, J. J. *Adv. Mater.* **1998**, *10*, 1461. Deumal, M.; Cirujeda, J.; Veciana, J.; Novoa, J. J. *Chem. Eur. J.* **1999**, *5*, 1631.

(34) The diamagnetic correction applied to the raw data was too large, as evidenced by the positive slope in the χT vs T data at high temperatures. Thus data fitting was restricted to a maximum temperature of 170 K in order to avoid severe skewing of the fit by this overcorrection.

$= -J\mathbf{S_1S_2}$), with a mean field approximation[35] in order to account for the decrease in χT at low temperature.

$$\chi' = \rho\frac{\chi}{1 - (2zJ'/Ng^2\beta^2)\chi} \text{ where } \chi = \frac{2Ng^2\beta^2}{kT[3 + \exp(-J/kT)]} \quad (3)$$

Data fitting ($g = 2.00$ fixed) yielded $\rho = 0.97$, $J = 19.3 \pm 1.7$ cm^{-1}, and $zJ' = 1.01 \pm 0.03$ cm^{-1}. The agreement factor for this fit was not particularly strong (a modest 0.02), which reflected the differences between fit and experimental data associated with an overcorrection for the diamagnetism of PVC. Nonetheless, the data analysis clearly demonstrate that the spins in **7b** are weakly ferromagnetically coupled, consistent with the *m*-phenylene topology.

Discussion

Understanding of intramolecular interactions between verdazyl chromophores in di- and polyradicals has lagged behind analogous investigations of nitroxide systems—in part because of long-term stability problems associated with some of the specific verdazyl substrates (**3a**−**c**, **4a**, **4c**), while other systems have not been studied in enough detail (**2a**,**b**). Verdazyl diradicals **7a** and **7b** are among the first to be comprehensively studied and the first based on the ubiquitous benzene spacer to be sufficiently stable to allow such studies to be undertaken.

Analysis of the intramolecular magnetic interactions between verdazyl radicals indicate that they conform to the general pattern established for benzene-linked diradicals: The para-substituted diradical has antiferromagnetic exchange coupling and the meta analogue is ferromagnetic in nature. The magnitude of the exchange interactions in both compounds is fairly weak, which is in accord with the relatively small spin density on the verdazyl carbon atom directly bound to the central benzene linker (see above). The confinement of the individual radical SOMOs to each radical site means the principal means for spin communication is via spin polarization effects. In this respect, the magnetic properties of these diradicals most closely resemble those of other diradicals which similarly have small spin density at the site of substitution, e.g., **11**[36] and **12**.[9,37]

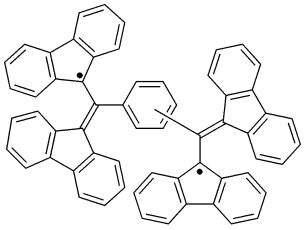

11

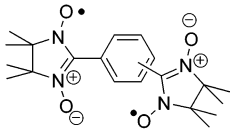

12

The nodal properties of the verdazyl SOMO have consequences for radical−radical communication as studied by methods other than magnetic ones. The isomeric diradicals have comparable electronic spectra (though as mentioned, interactions involving orbitals other than the SOMO are probably the reason for the differences in the higher energy absorptions), and in particular, the electrochemical properties of the two radicals are strikingly similar. The spin-state preferences of the diradicals appear to have no bearing on their redox processes. This is not unexpected because spin-state populations for these diradicals would not be observable at the ambient temperature conditions at which the electrochemical properties were studied. More unusual, however, is the observation that the two diradicals have essentially identical redox properties despite the different topologies and that for both diradicals the reduction and oxidation processes suggest *different* magnitudes of "electronic communication" *despite the fact that only one orbital*—the SOMO—is implicated for both processes. Clearly the notion of "electronic communication" in diradicals has to be thought about in different ways compared to bifunctional chromophores based on closed shell systems; in this context electrochemical studies of a wider range of neutral diradicals is a worthy area of study.

Experimental Section

1,3-Bis(1,5-diisopropyl-6-oxo-2,3,4,5-tetrazan-3-yl)benzene (6a). To a refluxing solution of 2,4-diisopropylcarbonohydrazide bis-hydrochloride[22] (1.00 g, 4 mmol), sodium acetate (0.67 g, 8 mmol), and methanol (75 mL) was added isophthalaldehyde (0.273 g, 2 mmol) in methanol (100 mL) dropwise over a period of 3 h. The solution was allowed to reflux in air for a further 20 h, at which time a pale yellow solution remained. The solvent was removed in vacuo and the residue dissolved in dichloromethane (5 × 50 mL). The dichloromethane fractions were then washed with distilled water (3 × 100 mL), dried with magnesium sulfate, and concentrated in vacuo yielding a pale yellow solid. The solid was then triturated with a minimal amount of ethyl acetate, ground into a fine powder, and heated in vacuo overnight at 90 °C affording **6a** as a white powder. Yield: 0.857 g, 95%. Mp: 180−182 °C dec. ^{1}H NMR (DMSO-d_6): δ 7.77 (s, 1H), 7.55 (d, 2H, ^3J = 8 Hz), 7.42 (t, 1H, ^3J = 7 Hz), 5.01 (d, 4H, ^3J = 11 Hz), 4.49 (sep, 4H, ^3J = 8 Hz), 4.39 (t, 2H, ^3J = 11 Hz), 1.06 (d, 12H, ^3J = 7 Hz), 1.04 (d, 12H, ^3J = 7 Hz). ^{13}C NMR (DMSO-d_6): δ 153.5, 136.7, 128.3, 126.4, 125.5, 71.5, 46.7, 19.6, 18.5. FT-IR (KBr): 3245 (m) (NH), 1606 (s) (C═O) cm^{-1}. MS (LSIMS): *m*/*z* 447 (M + H$^+$, 100). Anal. Calcd for $C_{22}H_{38}N_8O_2$: C, 59.17; H, 8.58; N, 25.09. Found: C, 59.09; H, 8.42; N, 24.83.

1,4-Bis(1,5-diisopropyl-6-oxo-2,3,4,5-tetrazan-3-yl)benzene (6b). To a refluxing solution of 2,4-diisopropylcarbonohydrazide bis-hydrochloride[22] (1.00 g, 4 mmol), sodium acetate (0.67 g, 8 mmol), and methanol (75 mL) was added terephthalaldehyde (0.273 g, 2 mmol) in methanol (100 mL) dropwise over a period of 3 h. The solution was left to reflux in air for a further 20 h at which time a pale yellow solution remained. The solvent was removed in vacuo and the residue dissolved in dichloromethane (5 × 50 mL). The dichloromethane fractions were then washed with distilled water (3 × 100 mL), dried with magnesium sulfate, and concentrated in vacuo yielding a pale yellow solid. The solid was then triturated with a minimal amount of ethyl acetate, ground into a fine powder, and heated in vacuo overnight at 90 °C affording **6b** as a white powder. Yield: 0.655 g, 73%. Mp: 162−164 °C dec. ^{1}H NMR (DMSO-d_6): δ 7.56 (s, 4H), 4.98 (d, 4H, ^3J = 11 Hz), 4.49 (sep, 4H, ^3J = 8 Hz), 4.34 (t, 2H, ^3J = 11 Hz), 1.05 (d, 12H, ^3J = 7 Hz), 1.03 (d, 12H, ^3J = 7 Hz). ^{13}C NMR (DMSO-d_6): δ 153.5, 136.6, 126.7, 71.5, 46.8, 19.6, 18.4. FT-IR (KBr): 3245 (m) (NH), 1610 (s) (C═O) cm^{-1}. MS (LSIMS): *m*/*z* 447 (M + H$^+$, 100). Anal. Calcd for $C_{22}H_{38}N_8O_2$: C, 59.17; H, 8.58; N, 25.09. Found: C, 59.26, H, 8.22; N, 24.86.

1,3-Bis(1,5-diisopropyl-6-oxo-3-verdazyl)benzene (7a). A solution of **6a** (0.300 g, 0.67 mmol), benzoquinone (0.220 g, 2.0 mmol), and toluene (20 mL) was allowed to reflux for 30 min in air before being taken to dryness in vacuo. The residue was purified via column chromatography (5 × 20 cm neutral alumina, dichloromethane) before it was once again taken to dryness. The purified

(35) Carlin, R. L. *Magnetochemistry*; Springer-Verlag: New York, 1986.
(36) (a) Tukada, H. *J. Am. Chem. Soc.* **1991**, *113*, 8991. Tukada, H.; Mutai, K. *Tet. Lett.* **1992**, *33*, 6665.
(37) Caneschi, A.; Chiesi, P.; David, L.; Ferraro, F.; Gatteschi, D.; Sessoli, R. *Inorg. Chem.* **1993**, *32*, 1445.

residue was recrystallized via slow cooling of a saturated ethyl acetate solution affording **7a** as well formed orange-red crystals suitable for X-ray crystallography. Yield: 0.184 g, 62%. Mp: 134−136 °C dec. FT-IR (KBr): 1675 (s) (C═O) cm^{-1}. UV−vis (CH_2Cl_2): λ_{max} 248 nm (ϵ = 48500), 417 nm (ϵ = 3018), 480 nm (ϵ = 980). MS (EI): *m*/*z* 440 (M^+, 100). Anal. Calcd for $C_{22}H_{32}N_8O_2$: C, 59.98; H, 7.32; N, 25.44. Found: C, 60.21; H, 7.26; N, 25.51.

1,4-Bis(1,5-diisopropyl-6-oxo-3-verdazyl)benzene (7b). A solution of **6b** (0.300 g, 0.67 mmol), benzoquinone (0.220 g, 2.0 mmol), and toluene (20 mL) was allowed to reflux for 30 min in air before being taken to dryness in vacuo. The residue was purified via column chromatography (5 cm × 20 cm neutral alumina, dichloromethane) before it was once again taken to dryness. The purified residue was recrystallized via slow cooling of a saturated ethyl acetate solution affording **7b** as well formed orange-red crystals suitable for X-ray crystallography. Yield: 0.194 g, 66%. Mp: 160−162 °C. FT-IR (KBr): 1678 (s) (C═O) cm^{-1}. UV−vis (CH_2Cl_2): λ_{max} 280 nm (ϵ = 46300), 417 nm (ϵ = 3090), 485 nm (ϵ = 1000). MS (EI): *m*/*z* 440 (M^+, 100). Anal. Calcd for $C_{22}H_{32}N_8O_2$: C, 59.98; H, 7.32; N, 25.44. Found: C, 60.00; H, 7.10; N, 25.51.

1,5-Diisopropyl-3-phenyl-1,2,4,5-tetrazane 6-Oxide (8). 2,4-Diisopropylcarbonohydrazide bishydrochloride[22] (2.39 g, 9.63 mmol), sodium acetate (1.58 g, 19.3 mmol), and benzaldehyde (0.99 mL, 9.6 mmol) were combined in ethanol (200 mL) and refluxed overnight. The solution was filtered and the solvent removed under reduced pressure. The crude product was recrystallized from heptane to give **8** as a white microcrystalline solid. Yield: 1.7 g, 67%. Mp: 126−128 °C. ^{1}H NMR ($CDCl_3$): δ 7.57 (d, 2H, ^3J = 7 Hz), 7.38 (m, 3H), 4.66 (septet, 2H, ^3J = 7 Hz), 4.58 (t, 1H, ^3J = 12 Hz), 3.75 (d, 2H, ^3J = 12 Hz), 1.14 (d, 6H, ^3J = 7 Hz), 1.12 (d, 6H, ^3J = 7 Hz). ^{13}C NMR ($CDCl_3$): δ 154.5, 135.9, 129.0, 128.9, 126.4, 71.2, 48.0, 19.8, 18.6. FT-IR (KBr): 3216 (m) (NH), 1587 (s) (C═O) cm^{-1}. MS (EI): *m*/*z* 262 (M^+, 23). Anal. Calcd for $C_{14}H_{22}N_4O$: C, 64.09; H, 8.45; N, 21.36. Found: C, 64.22; H, 8.24; N, 21.24.

1,5-Diisopropyl-3-phenyl-6-oxoverdazyl (9). *p*-Benzoquinone (0.66 g, 6.1 mmol) was added to a solution of 1,5-diisopropyl-3-phenyl-1,2,4,5-tetrazane 6-oxide **8** (1.07 g, 4.08 mmol) in toluene (50 mL), and the mixture was refluxed for 1 h. The solution was filtered to remove crystallized hydroquinone before the solvent was removed under reduced pressure. The oily red product was purified by flash chromatography (CH_2Cl_2, alumina) to give **9** as a red oil that solidified upon sitting. Yield: 0.79 g, 75%. Mp: 50−52 °C. FT-IR (KBr): 1680 (s) (C═O) cm^{-1}. UV−vis (CH_2Cl_2): λ_{max} 249 nm (ϵ = 32375), 414 nm (ϵ = 1925). MS (EI) *m*/*z* 259 (M^+, 16). Anal. Calld for $C_{14}H_{19}N_4O$: C, 64.84; H, 7.38; N, 21.60. Found: C, 64.02; H, 7.21; N, 21.87.

Acknowledgment. We thank the University of Victoria and the Natural Sciences and Engineering Research Council of Canada for financial support. We also thank Dr. Natia L. Frank for helpful discussions.

Supporting Information Available: General experimental section and characterization details for all new compounds. This material is available free of charge via the Internet at http://pubs.acs.org.

JO7014449